

# Impacts of electronically photo-excited NO<sub>2</sub> on air pollution in the South Coast Air Basin of California

J. J. Ensberg<sup>1,\*</sup>, M. Carreras-Sospedra<sup>1</sup>, and D. Dabdub<sup>1</sup>

<sup>1</sup>Department of Mechanical and Aerospace Engineering, University of California at Irvine, Irvine, California, USA

\*now at: the California Institute of Technology, Pasadena, California, USA

Received: 8 August 2009 – Published in Atmos. Chem. Phys. Discuss.: 11 September 2009

Revised: 13 January 2010 – Accepted: 13 January 2010 – Published: 3 February 2010

**Abstract.** A new path for hydroxyl radical formation via photo-excitation of nitrogen dioxide (NO<sub>2</sub>) and the reaction of photo-excited NO<sub>2</sub> with water is evaluated using the UCI-CIT model for the South Coast Air Basin of California (SoCAB). Two separate studies predict different reaction rates, which differ by nearly an order of magnitude, for the reaction of photo-excited NO<sub>2</sub> with water. Impacts of this new chemical mechanism on ozone and particulate matter formation, while utilizing both reaction rates, are quantified by simulating two summer episodes. First, sensitivity simulations are conducted to evaluate the uncertainty in the rate of reaction of photo-excited NO<sub>2</sub> with water reported in the literature. Results indicate that the addition of photo-excited NO<sub>2</sub> chemistry increases peak 8-h average ozone and particulate matter concentrations.

The importance of this new chemistry is then evaluated in the context of pollution control strategies. A series of simulations are conducted to generate isopleths for ozone and particulate matter concentrations, varying baseline nitrogen oxides (NO<sub>x</sub>) and volatile organic compounds (VOC) emissions. Isopleths are obtained using 1987 emissions, to represent past conditions, and 2005, to represent current conditions in the SoCAB. Results show that the sensitivity of modeled pollutant control strategies due to photoexcitation decreases with the decrease in baseline emissions from 1987 to 2005. Results show that including NO<sub>2</sub> photo-excitation, increases the sensitivity of ozone concentration with respect to changes in NO<sub>x</sub> emissions for both years. In particular, decreasing NO<sub>x</sub> emissions in 2005 when NO<sub>2</sub> photo-excitation is included, while utilizing the higher reaction rate, leads to ozone relative reduction factors that are 15% lower than in a case without photo-excited NO<sub>2</sub>. This implies that photoexcitation increases the effectiveness in reducing ozone through

NO<sub>x</sub> emissions reductions alone, which has implications for the assessment of future emission control strategies. However, there is still disagreement with respect to the reaction rate constant for the formation of OH. Therefore, further studies are required to reduce the uncertainty in the reaction rate constant before this new mechanism is fully implemented in regulatory applications.

## 1 Introduction

The hydroxyl radical (OH) is one of the most important oxidants in the troposphere during daylight hours. It oxidizes volatile organic compounds (VOCs) and participates in the catalytic cycle of ozone formation. In remote areas, OH is produced via photolysis of ozone (O<sub>3</sub>) in the presence of water. In polluted atmospheres, OH is also formed by the photolysis of nitrous acid (HONO) and hydrogen peroxide (H<sub>2</sub>O<sub>2</sub>). In addition, OH is formed through reaction of hydroperoxy radical (HO<sub>2</sub>) and nitrous oxide. Hence, sources of HO<sub>2</sub> are eventual sources of OH. All these reactions have been long recognized as the major formation paths of OH and ozone.

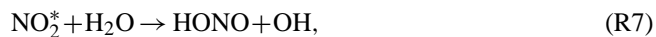


where  $h$  is Planck's constant and  $\nu$  is a photon of light with wavelength  $\lambda$ . A recent study by Li et al. (2008) suggested that an additional source of OH could contribute significantly



Correspondence to: D. Dabdub  
(ddabdub@uci.edu)

to OH formation. The new OH production mechanism is as follows:



where M is either an O<sub>2</sub> or N<sub>2</sub> molecule. Reaction (R6) occurs for  $\lambda > 400$  nm. For  $\lambda < 400$  nm, NO<sub>2</sub> dissociates into NO and O(<sup>3</sup>P). A previous study by Crowley and Carl (1997), analyzed the yield of Reaction (R7), and suggested that this new mechanism has a limited impact on the OH formation. In contrast to these results, the study by Li et al. (2008) reported a reaction rate for Reaction (R7) to be an order of magnitude higher than that found by Crowley and Carl (1997). Despite the ambiguity as to the appropriate reaction rate to associate with Reaction (R7), both Li et al. (2008) and Crowley and Carl (1997) show that Reactions (R6–R8) have the potential to increase the amount of OH which is produced in the troposphere. Given the dependence of ozone production on OH concentrations in urban areas, the increase in OH due to Reaction (R7) must be considered when simulating ozone formation and formulating ozone control strategies.

Traditional control strategies for ozone focus on reducing NO and NO<sub>2</sub> (together known as NO<sub>x</sub>) as well as VOC emissions. In conjunction with sunlight, OH, NO<sub>x</sub> and VOC mixing ratios play a key role in the amount of ozone that is produced throughout the day. Ozone control strategies are based on previous experimental and numerical studies and most, for the South Coast Air Basin of California (SoCAB), focus on reducing VOC emissions more aggressively than NO<sub>x</sub> emissions (Chock et al., 1999; Meng et al., 1997; Milford et al., 1994). Some studies that analyzed weekday to weekend differences in NO<sub>x</sub>, VOC, and ozone levels suggest that in areas where NO<sub>x</sub> emissions are high, such as the SoCAB, decreasing NO<sub>x</sub> emissions may increase peak ozone concentrations. This is due to a decrease in the yield of the termination reaction of NO<sub>2</sub> with OH to produce nitric acid and of the titration of O<sub>3</sub> by NO, both decreases caused by decreasing NO<sub>x</sub> emissions (Qin et al., 2004; Blanchard and Tanenbaum, 2003; Chinkin et al., 2003; Fujita et al., 2003). Reactions (R6–R8) affect the ambient ozone concentrations as reported by Wennberg and Dabdub (2008) and Sarwar et al. (2009). Because the yield of Reactions (R6–R8) depends on NO<sub>x</sub> levels, the effect of photoexcitation on emission control strategies should be evaluated to determine if the reactions alter the effectiveness of emission controls.

There are two main objectives in this study. The first objective of this study is to analyze the effect of including NO<sub>2</sub> photo-excitation processes in a three-dimensional air quality model using a well-studied episode that represents emissions from 1987. The second objective of this study is to determine how the addition of Reactions (R6–R8) affects air pollution control strategies using two differentiated emissions episodes

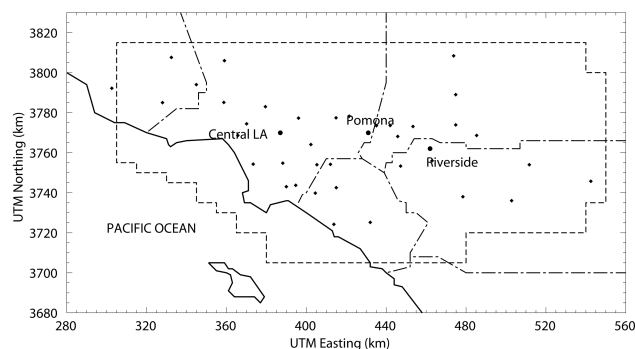


**Fig. 1.** Model domain of the UCI-CIT air quality model. The map shows the location of Central Los Angeles, Pomona, and Riverside (shown in circles), which are the primary locations of interest for this analysis. Measurements from additional locations (shown in diamonds) were used to perform a statistical analysis of model accuracy.

for 1987 and 2005. These two episodes serve as sensitivity tests to evaluate photoexcitation with respect changes in baseline emission changes. The results show the sensitivity of NO<sub>2</sub><sup>\*</sup> on ozone control strategies as well as potential effects on particulate matter concentrations.

## 2 Methodology

Three dimensional air-quality models have become the status quo for determining the impacts of newly discovered chemical reactions on pollution control strategies. Numerical simulations for this study are performed using the UCI-CIT Airshed Model (Harley et al., 1993; Griffin et al., 2002). The UCI-CIT model was developed at the California Institute of Technology and continues to be upgraded by the Computational Environmental Sciences Laboratory (CESLab) at the University of California, Irvine. The modeling domain used for this study is presented in Fig. 1. The chemical mechanism used in the model is the Caltech Atmospheric Chemical Mechanism (CACM, Griffin et al., 2002) which stems from the SAPRC-99 chemical mechanism (Carter, 2000), and it contains detailed treatment of VOC oxidation to characterize secondary organic aerosol formation.

The model domain represents the South Coast Air Basin of California, which typically experiences the worst air quality of the United States. Hence, although it is a small area, it is of great interest, and has been studied in numerous efforts (Harley et al., 1993; Winner et al., 1995; Meng et al., 1997; Griffin et al., 2002). The typically high emissions of NO<sub>x</sub> in this area constitute an important factor for the study of NO<sub>2</sub> photoexcitation. Even though the spatial extent of the basin limits the generalization of the results, the high NO<sub>x</sub> emissions and intense insolation experienced in the area could be considered as parameters for an upper bound for the effects of NO<sub>2</sub> photoexcitation on O<sub>3</sub>.

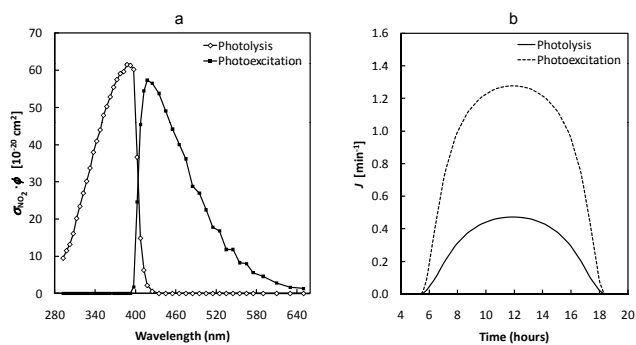


**Fig. 2.** (a) Absorption spectrum ( $\sigma$ ) of NO<sub>2</sub> times the quantum yield ( $\phi$ ) of NO<sub>2</sub> photolysis (hollow diamonds) and NO<sub>2</sub> photoexcitation (solid squares), (b) Rate of photolysis (solid line) and photoexcitation (dotted line) as a function of hour of the day, for 28 August 1987, in Los Angeles.

## 2.1 Model formulation

The photoexcitation reaction rate is derived from the absorption spectrum of NO<sub>2</sub> (Finlayson-Pitts and Pitts, 2000a). For the NO<sub>2</sub> photolysis, the quantum yield of the reaction ( $\phi_{\text{photolysis}}$ ) is one from 290 nm to 400 nm and decreases rapidly to zero from 400 nm to 420 nm. It is assumed that all NO<sub>2</sub> radiated by sunlight is photoexcited, and from the wavelength range of 290 nm to 420 nm, NO<sub>2</sub><sup>\*</sup> is completely dissociated into NO and O<sup>3</sup>P. Then, the effective quantum yield for NO<sub>2</sub><sup>\*</sup> formation is  $1 - \phi_{\text{photolysis}}$ , and hence, formation of NO<sub>2</sub><sup>\*</sup> occurs at wavelengths longer than 420 nm (see Fig. 2a). As for all photolysis reactions, NO<sub>2</sub> photolysis and photoexcitation depend on the solar zenith angle, which is a function of the latitude, the time of the year, and the time of the day. For Los Angeles, in 27 August, the variation of the photolysis and photoexcitation rates during the day is shown in Fig. 2b. The rate of photoexcitation is 3–4 times higher than the photolysis of NO<sub>2</sub>, which is consistent with values presented by Crowley and Carl (1997). The quenching rate constants for Reaction (R8) have been measured as  $2.7 \times 10^{-11}$ ,  $3.0 \times 10^{-11}$ , and  $1.7 \times 10^{-10} \text{ cm}^3 \text{ molecule}^{-1} \text{ s}^{-1}$  for N<sub>2</sub>, O<sub>2</sub>, and H<sub>2</sub>O, respectively. Even though the photoexcitation reaction is faster than photolysis, rapid quenching of NO<sub>2</sub><sup>\*</sup> limits the overall consumption of NO<sub>2</sub> through Reactions (R6–R8) to be  $10^{-4}$  times slower than NO<sub>2</sub> photolysis.

## 2.2 Model evaluation for new chemical mechanism

The first objective of the study is to determine the effect of NO<sub>2</sub> photoexcitation using a well-studied episode of ozone formation in 1987. The scientific literature reports two different reaction rates associated with Reaction (R7), which are shown in Table 1. Therefore, this study explores the sensitivity of ozone formation with respect to both reaction rates. Three simulated cases are compared to meteorological and air quality data measured by the California Air Resources

**Table 1.** Reaction rates for photo-excited NO<sub>2</sub> reacting with H<sub>2</sub>O are presented. High and low reaction rates correspond to the reaction rates determined experimentally by Li et al. (2008) and Crowley and Carl (1997), respectively.

Simulated Case	Reaction Rate (Reaction R7)
Base Case	No photo-excited NO <sub>2</sub> chemistry
Low Reaction Rate Case	$1.2 \times 10^{-14} \text{ cm}^3 \text{ molecule}^{-1} \text{ s}^{-1}$
High Reaction Rate Case	$1.7 \times 10^{-13} \text{ cm}^3 \text{ molecule}^{-1} \text{ s}^{-1}$

Board (ARB) on 27–28 August 1987. Data were collected as part of the Southern California Air Quality Study (SCAQS) and have been used extensively to validate air quality models in other studies (Meng et al., 1997; Griffin et al., 2002). In addition, Zeldin et al. (1990) indicated that 28 August 1987 is representative of the meteorological conditions in the South Coast Air Basin of California, which makes it suitable for modeling an air quality episode. Hence, meteorological and air quality data for 27–28 August are used as the basis for the assessment of the impact of the photo-excitation processes on ozone and particulate matter control dynamics. The meteorological conditions of the episode are expected to facilitate the extent of the photoexcitation reaction, and hence, provide meteorological conditions for the upper bound for NO<sub>2</sub> photoexcitation and its effects on ozone formation. Maximum particulate matter concentrations in the South Coast Air Basin occur generally in late fall months, but the impact of NO<sub>2</sub> photoexcitation during that time of the year is limited by the lower insolation with respect to summer months. As a result, impacts on PM under summer conditions presented here represent an upper bound for the effects of NO<sub>2</sub> photoexcitation on secondary PM.

The three simulated cases include: (i) the UCI-CIT Airshed Model's base case, which does not include Reactions (R6–R8), (ii) a case which includes the new chemistry while utilizing Li et al.'s (2008) high reaction rate for Reaction (R7), hence referred to as the “high reaction rate case”, and (iii) a case which includes the new chemistry while utilizing Crowley and Carl's low reaction rate for Reaction (R7), hence referred to as the “low reaction rate case”. The three simulated cases are summarized in Table 1.

Model performance for the three cases is evaluated against observations using typical statistical norms, as described by Russell and Dennis (2000), which were used previously to assess model performance and its representation of secondary organic aerosols (Griffin et al., 2002).

## 2.3 Effect of emission changes

The second objective of this study is to assess the sensitivity of ozone and PM control strategies to NO<sub>2</sub> photoexcitation, using past emissions represented by 1987 emissions and

current emissions levels represented by 2005 emissions. Previous studies have attempted to quantify the effects of altering NO<sub>x</sub> and VOC emission scaling factors on the formation of aerosol pollutants and the reduction of ozone (Winner et al., 1995; Meng et al., 1997; Nguyen and Dabdub, 2002). In this study, multiple day summer smog episodes are simulated while accounting for all feasible combinations of NO<sub>x</sub> and VOC emission ratios.

For the case with 1987 emissions, all three NO<sub>2</sub> photoexcitation cases – base case, low and high reaction rate cases – emissions of NO<sub>x</sub> and VOC emissions are amplified by factors of 0.0, 0.4, 0.8, 1.0, 1.2, and 1.6 throughout the domain of the model. Simulation results are incorporated in isopleth charts to illustrate the dynamics of emission reductions. This study focuses on isopleths constructed for each of the three reaction rate cases using peak 8-h average ozone concentration and 24-h average PM<sub>10</sub> concentration at selected locations. The impact of the new chemistry on emission reductions is then evaluated by calculating the difference between isopleths resulting from including Reactions (R6–R8) at specific locations and the base case.

Anthropogenic emissions have declined dramatically since 1987. From 1985 to 2005 emissions of NO<sub>x</sub> and reactive organic gases decreased by 37% and 66%, respectively (CARB, 2009). Hence, assessing the effects of NO<sub>2</sub> photoexcitation on future emission control strategies requires the analysis of more recent emissions than the ones estimated for 1987. Consequently, the effect of photoexcitation on future emission control strategies is evaluated using an emissions inventory for the year 2005, which was developed for the 2007 Air Quality Management Plan by the South Coast Air Quality Management District (SCAQMD, 2007). Iso-pleths are constructed for the base case and the high reaction rate case. While the isopleths constructed using 2005 emissions illustrate near-current conditions in the South Coast Air Basin of California, the analysis conducted for the case of 1987 emissions illustrates the potential effect of photoexcitation in areas with high levels of NO<sub>x</sub> emissions, such as Mexico and megacities in China, as suggested by Sarwar et al. (2009).

## 3 Results

### 3.1 Baseline Air Quality Simulations

Baseline air quality simulations are conducted using 1987 emissions to assess the sensitivity of model performance with the addition of the new reactions. To reduce the effects of initial conditions on final concentrations, 27 and 28 August are first simulated excluding any aerosol phase chemistry. The final concentrations after these two days are then used as initial conditions for the same two-day simulation with aerosol phase chemistry included in the simulation. Previous studies have shown that this technique reduces irregularities caused

by initial conditions up to 90% after 2 days of simulation (Nguyen and Dabdub, 2002). The first set of two days is used to spin-up the effect of emissions and the photoexcitation reactions. Carreras-Sospedra et al. (2006) showed that it takes 2 days to minimize the effect of initial conditions in the South Coast Air Basin of California, under these meteorological conditions. The second set of two days is then used for analysis. Even though this approach does not represent a real 4-day episode, it serves the purpose to assess the impacts that the new mechanism has on baseline concentrations and emission controls during a high ozone forming conditions.

Since NO<sub>2</sub> photolyzes throughout the day to produce NO, it is important to analyze NO<sub>2</sub> and NO separately and not as NO<sub>x</sub>. Figure 3a–c shows the 1-h NO concentrations, resulting from the simulated cases together with measured concentrations in the cities of Los Angeles, Pomona, and Riverside for 27–28 August 1987. Figure 3d–f shows the simulated and measured 1-h average ozone concentrations for the same cities and period of time. Simulated results shown in Fig. 3 correspond to the three cases described above.

In general, changes in pollutant concentrations are attributed to the increase in OH concentration due to NO<sub>2</sub> photoexcitation. For typical O<sub>3</sub>, NO<sub>2</sub> and water concentrations in the year 1987 of 90 ppb, 50 ppb and 15 500 ppm, respectively, the instantaneous formation of OH through photoexcitation is nearly 6% of the OH formed through O<sub>3</sub> photolysis, using Li et al. value for Reaction (R7). The contribution of NO<sub>2</sub> photoexcitation to total OH formation is less than 0.4% using the reaction rate suggested by Crowley and Carl. Increases in OH concentrations can initiate more oxidation of organic compounds that can then react with NO to recycle NO<sub>2</sub> back. In addition, photoexcitation also contributes to the increase in HONO through Reaction (R8), and to the formation of nitric acid through Reaction (R9).



The incorporation of Reactions (R6–R8) results in a decrease in NO for Riverside throughout the two-day simulation. The maximum decrease in NO is 20 ppb, which occurs at hour 30 in the high reaction rate case. Similar trends in NO decreases occur in Los Angeles, although the differences are considerably smaller, with maximum decreases in NO concentrations less than 1–2 ppb. Pomona also exhibits similar trends in NO reduction with the inclusion of Reactions (R6–R8). The maximum decrease results at hour 41 and is close to 10 ppb. These decreases are due to the increase availability of radicals initiated by the increase in OH concentrations. Radical of organic compounds react with NO to recycle NO<sub>2</sub> back. As a result, NO concentrations using photoexcitation are lower than in the base case. Conversely, NO<sub>2</sub> concentrations increase with the addition of NO<sub>2</sub> photoexcitation (not shown). Impacts in pollutant concentrations are amplified by the use of the high reaction rate as opposed to the low reaction rate.

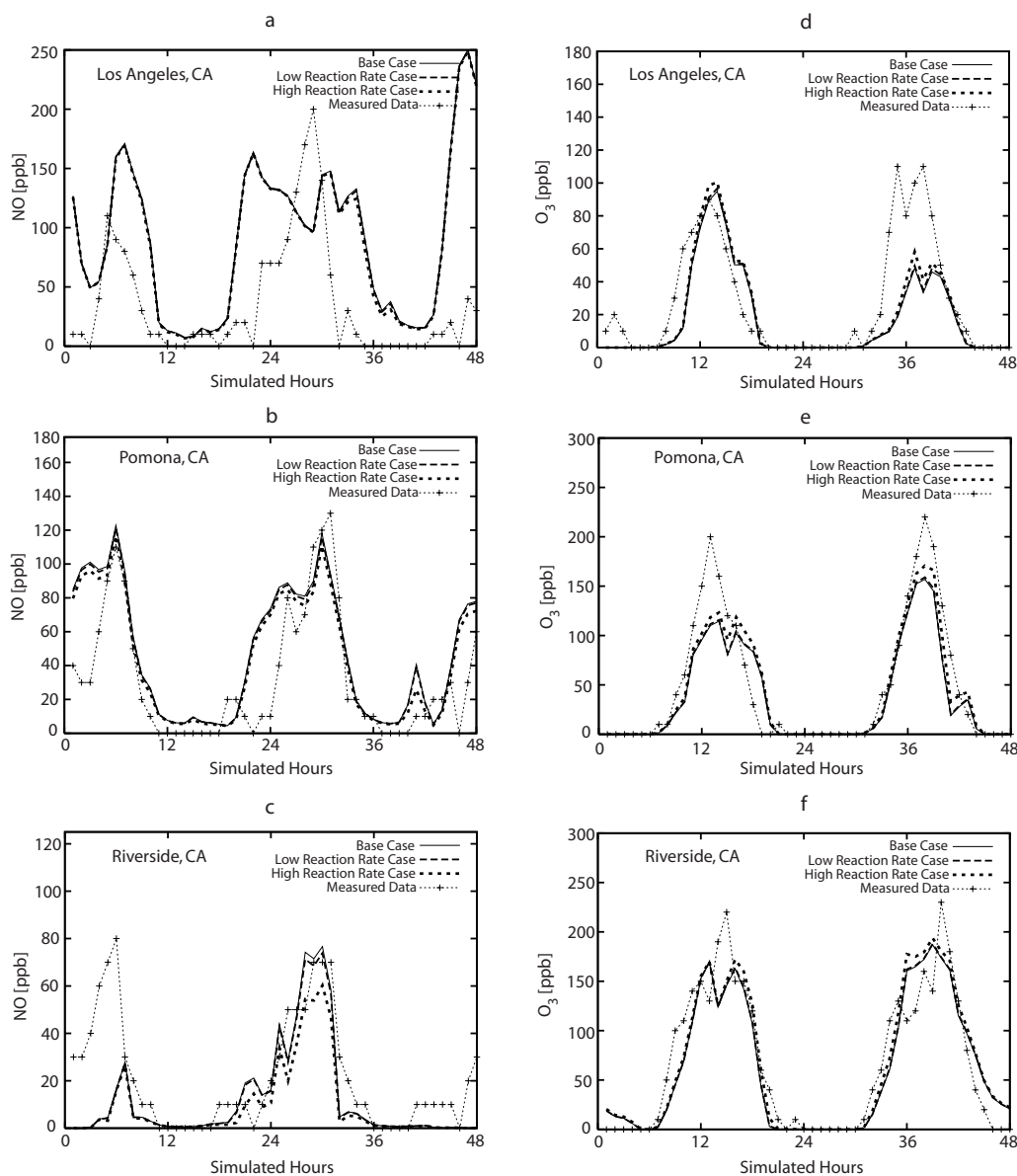


**Fig. 3.** Simulated and measured NO and ozone concentrations in the South Coast Air Basin of California for 27–28 August 1987. All figures depict four cases which include 1-h average concentrations for the UCI-CIT base case, 1-h average concentrations for a case with NO<sub>2</sub> photo-excitation chemistry utilizing the low reaction rate, (Crowley and Carl, 1997), 1-h average concentrations for a case with NO<sub>2</sub> photo-excitation chemistry utilizing the high reaction rate (Li et al., 2008), and measured concentrations from the California Air Resources Board (CARB, 2009b). The numerical values of the high and low reaction rates are shown in Table 1. Subfigures shown correspond to (a) NO in Los Angeles, (b) NO in Pomona, (c) NO in Riverside, (d) ozone in Los Angeles, (e) ozone in Pomona, and (f) ozone in Riverside. All concentrations are in ppb.

Ozone is one of the main pollutants of interest, and the resulting increases in ozone concentrations presented in Fig. 3d–f merit significant attention. In Los Angeles, Fig. 3d, the second simulated peak concentration, for both simulated cases are much lower than the measured values. However, the maximum increases in simulated ozone concentration due to Reactions (R6–R8) still occur at the peaks and are equal to 20 ppb. Measured ozone concentrations in Pomona,

Fig. 3e, during the first peak are close to 100 ppb higher than any predicted concentrations. The maximum differences between simulated concentrations and measured concentrations during the second peak decrease to 50 ppb, although there is a much stronger similarity in shape among all four cases. Similar trends in ozone increases occur in Riverside, Fig. 3f. By including Reactions (R6–R8) into the simulation, an increase in ozone production occurs during all daylight hours. The

high reaction rate results in the largest increases in ozone, with the maximum differences being approximately 10 ppb and occurring at the two peaks (hour 16 and hour 39). Although the simulated peak concentrations are significantly less than the measured peak concentrations at this location, there is still much overlap in the shape between all four cases throughout the 48 h simulation.

The model performance results for ozone and NO<sub>x</sub> for the base case and the cases with the addition of Reactions (R6–R8) are summarized in Table 2. In general, model performance is only affected slightly by the addition of the new reactions in terms of model error and bias, similarly to what Sarwar et al. (2009) reported. The most significant improvement in the model performance occurs for its total unpaired peak predictions of ozone concentrations.

Even though the model attains a better ozone peak prediction with the addition of NO<sub>2</sub> photoexcitation, there are many uncertainties that outweigh the importance of the NO<sub>2</sub> photoexcitation reaction. Rodriguez et al. 2003 presented the uncertainty analysis for the CACM mechanism in a box model, and suggested uncertainties of up to 44% in ozone concentration due to reaction rate constant uncertainties alone. Uncertainty in photolysis of NO<sub>2</sub> and aldehydes produced the highest model sensitivity. In addition, formation of nitric acid from NO<sub>2</sub> and OH, and the titration of ozone by NO also contribute to model uncertainty at low VOC-to-NO<sub>x</sub> ratios. For sensitivity of ozone formation due to model input uncertainties in a three-dimensional model, Rodriguez et al. (2007) suggested that NO<sub>x</sub> emissions are the highest contributor to model uncertainty when modeling ozone formation in the SoCAB, followed by VOC boundary conditions. In addition, ozone boundary conditions affect uncertainty in modeled ozone formation in coastal areas and the titration of ozone by NO contributes to ozone uncertainty in locations downwind from Los Angeles, such as Riverside. Carreras-Sospedra et al. (2006) reported sensitivity of the model to meteorological conditions and suggested a strong sensitivity of peak ozone concentration to temperature changes. Carreras-Sospedra et al. (2006) also reported increases in ozone peak concentrations of more than 100 ppb with respect to simulations with Urban Airshed Model (UAM) using the CBIV chemical mechanism.

Griffin et al. (2002) evaluated the UCI-CIT model using a different meteorological episode (8–9 September 1993), and they showed good agreement in selected locations in terms of total PM mass and species distribution in the aerosol. Nguyen and Dabdub (2002) reported measured nitrate PM<sub>2.5</sub> in Riverside, which is compared to simulated concentrations in Fig. 4. In general, nitrate concentrations increase at the peaks with the inclusion of NO<sub>2</sub> photoexcitation. Maximum increases in nitrate PM due to the high reaction rate case are up to 25% in Riverside.

Formation of NO<sub>2</sub><sup>\*</sup> also occur from the titration of NO with O<sub>3</sub> (Reaction R10), which has not been included in this study.

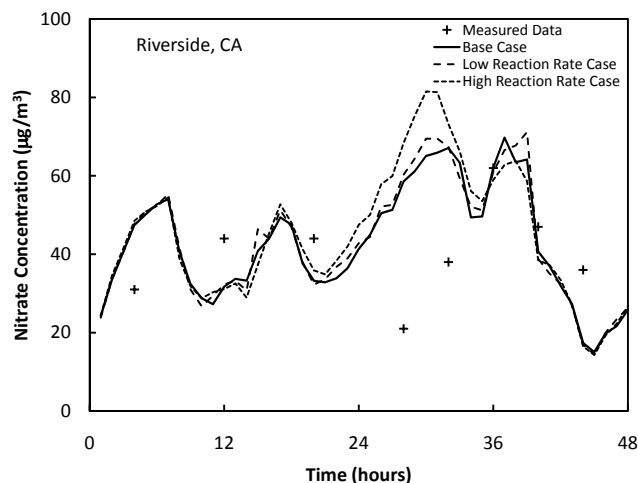


**Fig. 4.** Simulated and measured nitrate PM<sub>2.5</sub> in Riverside, California, for 27–28 August 1987. The figure depicts four cases which include 1-h average Nitrate PM<sub>2.5</sub> concentrations for the UCI-CIT base case, 1-h average Nitrate PM<sub>2.5</sub> concentrations for a case with NO<sub>2</sub> photo-excitation chemistry utilizing the low reaction rate (Crowley and Carl, 1997), 1-h average Nitrate PM<sub>2.5</sub> concentrations for a case with NO<sub>2</sub> photo-excitation chemistry utilizing the high reaction rate (Li et al., 2008), and measured concentrations reported by Nguyen and Dabdub (2002). The numerical values of the high and low reaction rates are shown in Table 1 of the manuscript.

NO<sub>2</sub><sup>\*</sup> formed from O<sub>3</sub> + NO is electronically excited ranging from 590 to 2800 nm (Finlayson-Pitts and Pitts, 2000b).



Assuming that all NO<sub>2</sub><sup>\*</sup> photo-excited at that wavelength range can react with water to form OH, the instantaneous rate of production of NO<sub>2</sub><sup>\*</sup> can be expressed as the sum of the rate of production of NO<sub>2</sub><sup>\*</sup> through Reactions (R6) and (R10). The peak formation of NO<sub>2</sub><sup>\*</sup> due to photoexcitation occurs at noon, when the solar intensity is the highest. Formation of NO<sub>2</sub><sup>\*</sup> due to ozone titration by NO peaks between the morning rush hours and noon, when ozone concentration starts to pick up due to higher solar intensity and concentrations of NO are still relatively high after the morning commute. In areas such as Los Angeles, with typical noon concentrations of NO, NO<sub>2</sub> and O<sub>3</sub> of 10, 30 and 40 ppb, respectively, the contribution of Reaction (R10) to total NO<sub>2</sub><sup>\*</sup> production is approximately 23%. Crowley and Carl (1997) suggested that titration of ozone could contribute to 10% of the total NO<sub>2</sub><sup>\*</sup> formation in remote atmospheres. This mechanism of NO<sub>2</sub><sup>\*</sup> production is not included in the analysis however. Therefore, the effects of Reaction (R7) on ozone concentrations could be larger than the suggested by this study.

All these factors contribute to model uncertainty, and as a result, improvement of model accuracy due to the addition of NO<sub>2</sub> photoexcitation could be circumstantial. In addition, new studies report significantly lower values for the rate of

**Table 2.** Statistical analysis of model performance by comparing measured ozone, NO, and NO<sub>2</sub> concentrations to those predicted by the UCI-CIT Airshed Model with and without NO<sub>2</sub> photo-excitation chemistry is presented. The low reaction rate case refers to utilizing the reaction rate found by Crowley and Carl for Reaction (R2). The high Reaction rate case refers to utilizing the reaction rate found by Li et al. (2008) for Reaction (R2).

	Base Case	Low Reaction Rate Case	High Reaction Rate Case
Ozone			
Normalized Gross Error*	46%	46%	46%
Normalized Bias*	−5%	−4%	2%
Maximum Unpaired Peak Prediction	15%	15%	20%
Total Unpaired Peak Prediction	−145%	−120%	−8%
NO			
Normalized Gross Error	74%	74%	75%
Normalized Bias	46%	44%	41%
NO <sub>2</sub>			
Normalized Gross Error	26%	26%	26%
Normalized Bias	−13%	−13%	−13%

\* Calculated for observed values of [O<sub>3</sub>] > 60 ppb.

Reaction (R7) (Carr et al. 2009). Consequently, the scientific community should reach a consensus before these new reactions are included in regulatory air quality models.

### 3.2 Sensitivity of ozone concentrations due to nitrogen dioxide photoexcitation

Los Angeles and Riverside have been the focus of several studies due to their notoriously poor air quality and high levels of NO<sub>x</sub> and VOC emissions. Isopleths created using peak 8-h average ozone concentrations in Los Angeles are considerably different than those for Riverside. This is primarily due to the differences in emissions between the two cities.

The resulting peak 8-h average ozone isopleths for Riverside using 1987 emissions are shown in Fig. 5a–c. Figure 5b shows the differences in ozone concentrations in Riverside between the low reaction rate case and the base case, whereas Fig. 5c presents the differences between the high reaction rate case and the base case. By including Reactions (R6–R8), Fig. 5b shows increases of 1–2 ppb for most of the grid, which represent an increase of less than 1% when compared to the base case concentrations. Figure 5c, which corresponds to the high reaction rate, shows significantly larger differences in ozone production. The peak ozone concentrations steadily increase with increasing NO<sub>x</sub> and VOC. For baseline emissions – NO<sub>x</sub> and VOC equal 1.0 – ozone concentrations increase by up to 10 ppb (~7%) due to photoexcitation. Maximum increases are nearly 20 ppb, and these increases occur in the region above NO<sub>x</sub> equal to 1.4 and VOC equal to 1.4. Effects of photoexcitation in Los Angeles are more moderate, because ozone concentrations in that area are affected by termination reactions due to high NO<sub>x</sub> emissions. The results obtained using the 1987 emissions are not relevant for current and future emission control strategies because emissions in the SoCAB have declined significantly

in the past two decades. However, these results are illustrative of other areas, such as Mexico or megacities in China, as suggested by Sarwar et al. (2009). In those regions, economic and industrial development is causing elevated pollutant emissions, which could be comparable to the pollutant levels existing in the SoCAB in the year 1987.

The isopleths generated with 2005 emissions correspond to control scenarios with recent emissions. Hence, these isopleths are more illustrative of potential effects of future emission controls in the SoCAB, compared to 1987 isopleths. Because effects of photoexcitation in the low reaction rate case using 1987 emissions show minor impacts, the effect of photoexcitation in 2005 is only analyzed for the high reaction rate case. The resulting peak 8-h average ozone isopleths for Central Los Angeles and Riverside are shown in Fig. 5d and g, respectively. Fig. 5e and h show the differences in peak 8-h average ozone concentrations between the high reaction rate case and the base case in Central Los Angeles and Riverside, respectively.

Ozone control strategies rely primarily on the variation of NO<sub>x</sub> and VOC emissions to abate ozone production. OH reacts with both NO<sub>x</sub> and VOC which is directly emitted or transported from upwind, to produce ozone. At high VOC to NO<sub>x</sub> ratios, reactions of VOC with OH dominate, which enhances the formation of ozone. At low VOC to NO<sub>x</sub> ratios, the reactions between NO<sub>x</sub> and OH dominate (Reaction R9), which is a termination reaction for ozone formation. In addition, NO<sub>x</sub> acts as a sink for ozone through direct titration (Reaction R10).

In the South Coast Air Basin of California, baseline NO<sub>x</sub> emissions are generally high, providing atmospheric conditions under low VOC to NO<sub>x</sub> ratios. Under these conditions, decreasing NO<sub>x</sub> alone leads to increases in ozone concentrations. For instance, it is well recognized that a major cause for having statistically higher ozone concentrations of ozone

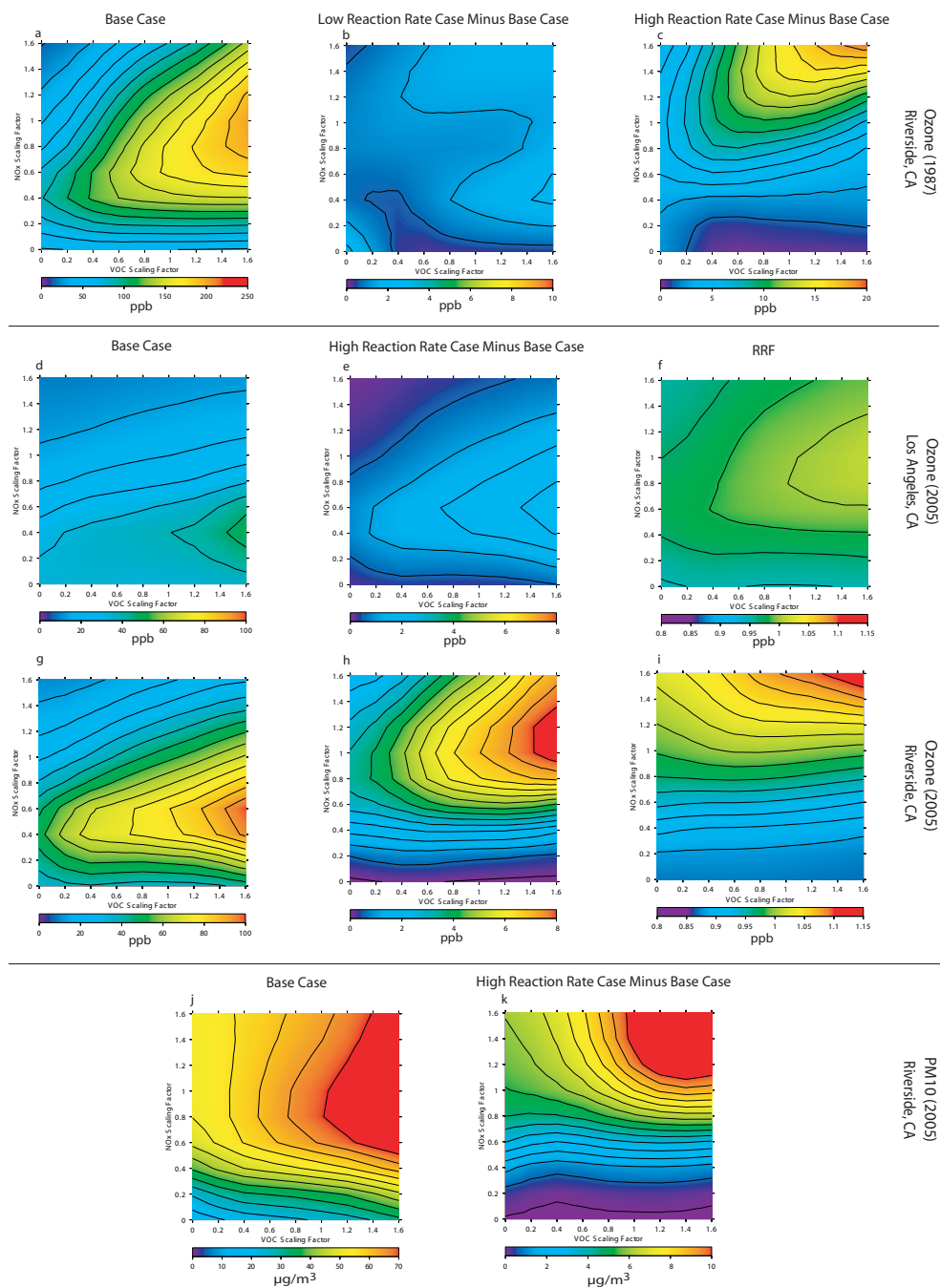


**Fig. 5.** Impact of NO<sub>2</sub> photo-excitation chemistry on ozone and PM<sub>10</sub> concentrations in the South Coast Air Basin of California: **(a)** Peak 8-h average ozone concentrations for base case in Riverside using 1987 emissions, **(b)** Peak 8-h average ozone concentrations for low reaction rate case minus those from base case in Riverside using 1987 emissions, **(c)** Peak 8-h average ozone concentrations for high reaction rate case minus those from base case in Riverside using 1987 emissions, **(d)** Peak 8-h average ozone concentrations for base case in Los Angeles using 2005 emissions, **(e)** Peak 8-h average ozone concentrations for high reaction rate case minus those from base case in Los Angeles using 2005 emissions, **(f)** ratio of Relative Reduction Factors (RRF) for high reaction rate case divided by RRF from base case in Los Angeles using 2005 emissions, **(g)** Peak 8-h average ozone concentrations for base case in Riverside using 2005 emissions, **(h)** Peak 8-h average ozone concentrations for high reaction rate case minus those from base case in Riverside using 2005 emissions, **(i)** ratio of RRF for high reaction rate case divided by RRF from base case in Riverside using 2005 emissions, **(j)** 24-h average PM<sub>10</sub> concentrations for base case in Riverside using 2005 emissions, **(k)** 24-h average PM<sub>10</sub> concentrations for high reaction rate case minus those from base case in Riverside using 2005 emissions. High and low reaction rates correspond to reaction rates of photo-excited NO<sub>2</sub> reacting with H<sub>2</sub>O determined experimentally by Li et al. (2008) and Crowley and Carl (1997), respectively. See Table 1 for numerical values of the reaction rates.

during the weekends in the South Coast Air Basin of California is the lower emissions of NO<sub>x</sub> with respect to weekdays, which reduces the yield of Reactions (R9–R10) (Qin et al., 2004; Blanchard and Tanenbaum, 2003; Chinkin et al., 2003; Fujita et al., 2003). The isopleths presented in Fig. 5a, d and g show that a decrease in NO<sub>x</sub> emissions of over 80% is necessary to achieve any decrease in ozone concentration, whereas moderate decreases in VOC emissions alone reduce ozone concentrations immediately.

The incorporation of Reactions (R6–R8) increases peak ozone concentrations in all locations under all NO<sub>x</sub> and VOC scaling factors. The increases in ozone concentrations occur because the mechanism provides an additional source of OH. The OH produced by the reaction of photo-excited NO<sub>2</sub> with water can then participate in the oxidation of another VOC molecule, increasing ozone production.

As shown in Fig. 5(e), in Los Angeles, the maximum increases in ozone concentration occur at NO<sub>x</sub> and VOC scaling factors of 0.6 and 1.6, respectively. At higher NO<sub>x</sub> scaling factors, the contribution of NO<sub>2</sub> photo-excitation to ozone production diminishes because the overall ozone formation is limited by the high emissions and the low VOC to NO<sub>x</sub> ratios. Conversely, in Riverside, the contribution of NO<sub>2</sub> photo-excitation to ozone formation increases with the increase in NO<sub>x</sub> scaling factors until  $f_{\text{NO}_x} = 1.2$  (Fig. 3(h)), because in these locations VOC to NO<sub>x</sub> ratios are higher than in Los Angeles. As a result, the increase in ozone production due to the new mechanism is not offset by the high level of NO<sub>x</sub> emissions, and hence, ozone concentrations in the high reaction rate case increase with respect to the base case, as the scaling factor for NO<sub>x</sub> increases.

In regulatory applications, the ratio of concentrations associated with future-year emissions-reduction and base-year emissions scenarios are used to scale the base-year ambient ozone design value to determine compliance with National Ambient Air Quality Standards (NAAQS). The use of those ratios, referred as relative reduction factors (RRF), minimizes the effect of model-to-model variations in model pollutant predictions. Hogrefe et al. (2008) demonstrate this point in a recent study, where they find marked model-to-model differences in ozone concentrations of up to 20 ppb, but only minor differences in the relative response of ozone concentrations to emission reductions. As a result, even though different models can differ in the prediction of absolute pollutant concentrations, the resulting RRF would lead to similar relative responses to air pollution control strategies.

In this study, RRF for a given pair of VOC and NO<sub>x</sub> reduction factors,  $\text{RRF}(f_{\text{VOC}}, f_{\text{NO}_x})$ , are calculated as the ratio of peak 8-hour average ozone concentration resulting for that particular pair ( $f_{\text{VOC}}, f_{\text{NO}_x}$ ) divided by peak 8-hour average ozone concentration for  $f_{\text{VOC}} = 1.0$  and  $f_{\text{NO}_x} = 1.0$ . Fig. 5f and i present the ratio of the RRF obtained with the high reaction rate case divided by the RRF obtained in the base case, for Central Los Angeles and Riverside, respectively.

For Central Los Angeles, maximum differences in RRF between the high reaction rate case and the base case are 5% or less. For Riverside, the high reaction rate case produces RRF that are up to 15% lower than in the base case for  $f_{\text{NO}_x} < 1$ , and RRF that are up to 15% higher than in the base case for  $f_{\text{NO}_x} > 1$ . Consequently, NO<sub>x</sub> emission controls simulated with NO<sub>2</sub> photoexcitation tend to produce more effective results than NO<sub>x</sub> emission controls simulated for the base case in terms of ozone concentrations. In contrast, for  $f_{\text{NO}_x} < 1$ , differences in RRF between the base case and the high reaction rate case are insensitive to VOC controls.

### 3.3 Sensitivity of PM concentrations due to nitrogen dioxide photoexcitation

Although ozone control strategies are the main consideration of this study, there are several other pollutants whose production is strongly connected to ozone production. These pollutants, such as particulate matter whose diameter is less than 10 μm (PM<sub>10</sub>) and particulate matter whose diameter is less than 2.5 μm (PM<sub>2.5</sub>), are strongly affected by including Reactions (R6–R8) into the model. Figure 5j shows isopleths of the 24-h average concentrations of PM<sub>10</sub> in Riverside for the base case using 2005 emissions. PM formation in the South Coast Air Basin of California is heavily influenced by nitrate dynamics. Peak PM concentrations have been measured consistently near the Riverside area, and are mostly composed of nitrate and ammonium. Nguyen and Dabdub (2002) confirmed such dynamics. Namely, high emissions of NO<sub>x</sub> oxidize to produce nitric acid that reacts with ammonia to produce ammonium nitrate. Because NO<sub>2</sub> photoexcitation leads to an increase in nitric acid production, concentration of nitrate in the aerosol increases by up to 14% with the addition of this new reaction. In contrast, the addition of photoexcitation leads to a slight decrease in the formation of secondary organic aerosol.

As discussed by Nguyen and Dabdub (2002), in the regime of low NO<sub>x</sub> scaling factors, formation of secondary particles increases linearly with the increase in NO<sub>x</sub> emissions. This increase is tightly related to the increase in ozone concentration shown in Fig. 5g. Increasing ozone concentration increases the formation of OH, via Reactions (R1–R2), which in turn can react with NO<sub>2</sub> to form nitric acid which eventually produces aerosols via Reaction (R11):



Under a regime of high NO<sub>x</sub> and low VOC scaling factors, NO<sub>x</sub> ends up removing O<sub>3</sub>, and hence, reduce OH and aerosol formation. At high NO<sub>x</sub> and VOC scaling factors, ozone concentrations are the highest, producing high levels of OH and particles. In addition, in this regime of high NO<sub>x</sub> and VOC, formation of particles also has significant contributions from the formation of N<sub>2</sub>O<sub>5</sub> at night by the reaction of ozone with NO<sub>x</sub> (as suggested by Nguyen and Dabdub,

2002). N<sub>2</sub>O<sub>5</sub> can then react with water to form nitric acid, which leads to the formation of particles.

As with ozone, the low reaction rate case results in small (~1.0%) increases in 24-h average PM<sub>10</sub> concentrations for all NO<sub>x</sub> and VOC scaling factors (not shown). In the high reaction rate case (see Fig. 3k), the addition of Reactions (R6–R8) leads to increases in 24-h average PM<sub>10</sub> concentrations of 12% for 2005 baseline emissions. For  $f_{\text{NO}_x} < 1$ , the differences in PM<sub>10</sub> concentrations are almost entirely dependent on NO<sub>x</sub> scaling factors. There are two main mechanisms that explain this behavior. First, the decrease in NO<sub>x</sub> decreases the potential formation of photo-excited NO<sub>2</sub>, which can then form less OH molecules that will end up forming aerosols. Second, particulate matter formation is tightly related to ozone, as more ozone photolyzes during the day to produce OH, or it reacts with NO<sub>x</sub> at night to produce N<sub>2</sub>O<sub>5</sub>.

Previously, Nguyen and Dabdub (2002) found that PM<sub>10</sub> formation in the SoCAB is significantly more sensitive to changes in ammonia emissions than to either VOC or NO<sub>x</sub> emissions. The results presented in this article, however, suggest that the addition of NO<sub>2</sub> photo-excitation could increase the sensitivity of particle formation to changes in NO<sub>x</sub> emissions. Namely, a decrease in NO<sub>x</sub> emissions would achieve a higher decrease in particle formation if photo-excitation of NO<sub>2</sub> were included. Therefore, Reactions (R6–R8) merit consideration for air quality models not only for the assessment of ozone formation, but also for the potential impacts of this mechanism in the formation of secondary particulate matter.

#### 4 Conclusion

This study incorporates a new alternative path of hydroxyl radical formation via electronic photo-excitation of NO<sub>2</sub> into the chemical mechanism of a three dimensional air quality model, and it includes the analysis of uncertainty associated with the reaction rate of electronically excited NO<sub>2</sub> with water to form OH, based on studies performed by Li et al. (2008) and Crowley and Carl (1997). Results are used to assess the effects of the new mechanism on ozone and particulate matter predictions and on the impacts of pollution control strategies in the South Coast Air Basin of California under past conditions, represented by 1987 emissions, and under current conditions, represented by 2005 emissions.

The sensitivity of ozone and particulate matter formation to the new chemical path are quantified by simulating a two-day summer episode in 1987. The resulting simulated concentrations for the high reaction rate case (based on Li et al., 2008), the low reaction rate case (based on Crowley and Carl, 1997), and the UCI-CIT base case are then compared statistically to measured concentrations. Results indicate the largest impacts of NO<sub>2</sub> photo-excitation on ozone concentrations occur at the peaks for all cases. In general, model error and bias for ozone predictions are not affected significantly

by the addition of the new reactions, although results show that substantial improvements occur for peak ozone predictions at each location in the high reaction rate case for the 1987 episode.

Results of emission control strategies using an episode with high emissions, represented by the 1987 episode, indicate that the impacts of NO<sub>2</sub> photo-excitation in the low reaction rate case are minor, whereas the high reaction rate case increases ozone peak 8-hour average concentrations by up to 20 ppb in Riverside. The effect of photoexcitation in pollutant controls under current emissions, represented by 2005 emissions, is less pronounced than in the 1987 case. Maximum increases in 8-h average ozone concentrations of 8 ppb occur in downwind cities with low NO<sub>x</sub> emissions and high VOC to NO<sub>x</sub> ratios, such as Riverside. In areas with high NO<sub>x</sub> emissions and low VOC to NO<sub>x</sub> ratios, such as Los Angeles, increases in peak 8-h ozone concentrations are less than 2 ppb. The analysis of relative reduction factors obtained from ozone isopleths reveals that the high reaction rate case tends to increase ozone sensitivity with changes in NO<sub>x</sub> emissions. Namely, photoexcitation increases RRF by 15% with increasing NO<sub>x</sub> emissions, and reduces RRF by up to 15% with decreasing NO<sub>x</sub> emissions. As a result, the addition of photoexcitation increases the effectiveness of reducing ozone concentration with NO<sub>x</sub> emission reductions. In contrast, RRF experience little change in sensitivity to VOC emissions. Daily average PM<sub>10</sub> concentrations in the high reaction rate case are up to 12% higher than in the base case for 2005. Also, at NO<sub>x</sub> scaling factors below 1.0, the differences in PM<sub>10</sub> concentrations are almost entirely independent of VOC scaling factors. The results presented in this article suggest that the addition of NO<sub>2</sub> photo-excitation increases the sensitivity of ozone and particle formation to changes in NO<sub>x</sub> emissions above what models without photo-excitation predict.

Ozone and particulate matter control strategies rely heavily on the variation of NO<sub>x</sub> and VOC emissions and the addition of the new chemical mechanism increases peak ozone concentrations in all locations under all NO<sub>x</sub> and VOC scaling factors while utilizing both reaction rates. However, there is still a large uncertainty as to what the true reaction rate is. This study and Wennberg and Dabdub, (2008) suggest that the reaction rate reported by Li et al. (2008) impact significantly ozone formation in a high NO<sub>x</sub> emissions scenario represented by 1987 emissions in the SoCAB. In addition, this study and another study by Sarwar et al. (2009) suggest that the impacts using the high reaction rate case are still considerable even with significantly lower emissions. On the other hand, the reaction rate suggested by Crowley and Carl (1997) and by a more recent study (Car et al., 2009) produces minimal differences in pollutant model predictions. Consequently, further experimental work must be conducted to reduce uncertainty in the reaction rate of Reaction (R7).

*Acknowledgements.* The authors would like to thank the Undergraduate Research Opportunities Program (UROP) at the University of California at Irvine for their support with this research project. Also, the authors would like to thank James Kelly and Ajith Kaduwela, from the California Air Resources Board, and the anonymous referees for their invaluable comments.

Edited by: J. H. Seinfeld

## References

- Blanchard, C. L. and Tanenbaum, S. J.: Differences between weekday and weekend air pollutant levels in southern California, *J. Air Waste Manage.*, 53, 816–828, 2003.
- CARB, California Air Resources Board: CEPAM: 2009 Almanac – Standard Emissions Tool, <http://www.arb.ca.gov/app/emsinv/fcemssumcat2009.php>, last access: January 2010, 2009a.
- CARB, California Air Resources Board: Database: California Air Quality Data – Selected Data Available for Download, <http://www.arb.ca.gov/aqd/aqcd/aqcdldd.htm>, last access: January 2010, 2009b.
- Carr, S., Heard, D. E., and Blitz, M. A.: Comment on "Atmospheric Hydroxyl Radical Production from Electronically Excited NO<sub>2</sub> and H<sub>2</sub>O", *Science*, 324(5925), doi:10.1126/science.1166669, 2009.
- Carreras-Sospedra, M., Dabdub, D., Rodriguez, M. and Brouwer, J.: Air Quality Modeling in the South Coast Air Basin of California: What do the numbers really mean?, *Air Waste Manage. Assoc.*, 56, 1184–1195, 2006.
- Carter, W. P. L.: Programs and Files Implementing the SAPRC-99 Mechanism and its Associated Emissions Processing Procedures for Models-3 and Other Regional Models, available at: <http://www.cert.ucr.edu/~carter/SAPRC99/s99files.htm>, last accessed: December 2009, 2000.
- Chinkin, L. R., Coe, D. L., Funk, T., Hafner, H., Roberts, P., Ryan, P., and Lawson, D.: Weekday versus weekend activity patterns for ozone precursor emissions in California's south coast air basin, *J. Air Waste Manage.*, 53, 829–843, 2003.
- Chock, D. P., Chang, T. Y., Winkler, S. L., and Nance, B. L.: The impact of an 8 h air quality standard on ROG and NO<sub>x</sub> controls in Southern California, *Atmos. Environ.*, 33, 2471–2485, 1999.
- Crowley, J. N. and Carl, S. A.: OH Formation in the Photoexcitation of NO<sub>2</sub> beyond the Dissociation Threshold in the Presence of Water Vapor, *J. Phys. Chem.*, 101, 4178–4184, 1997.
- Finlayson-Pitts, B. J. and Pitts Jr., J. N.: Chemistry of the Upper and Lower Atmosphere, Academic Press, San Diego, California, USA, 95–96, 2000a.
- Finlayson-Pitts, B. J., and Pitts Jr., J. N.: Chemistry of the Upper and Lower Atmosphere, Academic Press, San Diego, California, USA, 548–549, 2000.
- Fujita, E. M., Stockwell, W. R., Campbell, D. E., Keislar, R. E., and Lawson, D. R.: Evolution of the magnitude and spatial extent of the weekend ozone effect in California's south coast air basin, 1981–2000, *J. Air Waste Manage.*, 53, 802–815, 2003.
- Griffin, R. J., Dabdub, D., and Seinfeld, J. H.: Secondary organic aerosol 1. Atmospheric chemical mechanism for production of molecular constituents, *J. Geophys. Res.*, 107, 4332–4358, 2002.
- Harley, R. A., Russell, A. G., McRae, G. J., Cass, G. R., and Seinfeld, J. H.: Photochemical Modeling of the Southern California Air Quality Study, *Environ. Sci. Technol.*, 27, 378–388, 1993.
- Hogrefe, C., Civerolo, K. L., Hao, W., Ku, J. Y., Zalewsky, E. E., and Sistla, G.: Rethinking the assessment of photochemical modeling systems in air quality planning applications, *J. Air Waste Manage. Assoc.*, 58, 1086–1099, 2008.
- Li, S., Matthews, J., and Sinha, A.: Atmospheric Hydroxyl Radical Production from Electronically Excited NO<sub>2</sub> and H<sub>2</sub>O, *Science*, 319, 1657–1660, 2008.
- Meng, Z., Dabdub, D., and Seinfeld, J. H.: Chemical Coupling Between Atmospheric Ozone and Particulate Matter, *Science*, 277, 116–119, 1997.
- Milford, J. B., Gao, D., Sillman, S., Blossey, P., and Russell, A. G.: Total Reactive Nitrogen (NO<sub>y</sub>) as an Indicator of the Sensitivity of Ozone to Reductions in Hydrocarbon and NO<sub>x</sub> Emissions, *Journal of Geophysical Research*, 99D, 3533–3542, 1994.
- Nguyen, K. and Dabdub, D.: NO<sub>x</sub> and VOC control and its effect on the formation of aerosols, *Aerosol Sci. Technol.*, 36, 560–572, 2002.
- Qin, Y., Tonnesen, G. S., and Wang, Z.: Weekend/weekday differences of ozone, NO<sub>x</sub>, CO, VOCs, PM<sub>10</sub> and the light scatter during ozone season in southern California, *Atmos. Environ.*, 38, 3069–3087, 2004.
- Rodriguez, M. A., Brouwer, J., Samuelsen, G. S., and Dabdub D.: Air quality impacts of distributed power generation in the South Coast Air Basin of California 2: Model uncertainty and sensitivity analysis, *Atmos. Environ.*, 41, 5618–5635, 2007.
- Rodriguez, M. and Dabdub, D.: Monte Carlo uncertainty and sensitivity analysis of the CACM chemical mechanism, *J. Geophys. Res.*, 108(D15), 4443, doi:10.1029/2002JD003281, 2003.
- Russell, A. and Dennis, R.: NARSTO critical review of photochemical models and modeling, *Atmos. Environ.*, 34, 2283–2324, 2000.
- Sarwar, G., Pinder, R. W., Appel, K. W., Mathur, R., and Carlton, A. G.: Examination of the impact of photoexcited NO<sub>2</sub> chemistry on regional air quality, *Atmos. Environ.*, 43, 6383–6387, 2009.
- South Coast Air Quality Management District of California (SCAQMD): Final 2007 Air Quality Management Plan, available at: <http://www.aqmd.gov/aqmp/07aqmp/index.html>, last access: December 2009, June 2007.
- Wennberg, P. O. and Dabdub, D.: Atmospheric chemistry - Rethinking ozone production. *Science*, 319, 1624–1625, 2008.
- Winner, D. A., Cass, G. R., and Harley, R. A.: Effect of alternative boundary conditions on predicted ozone control strategy performance: a case study in the Los Angeles area, *Atmos. Environ.*, 29, 3451–3464, 1995.
- Zeldin, M. D., Bregman, L. D., and Horie, Y.: A Meteorological and air quality assessment of the representativeness of the 1987 SCAQS Intensive Days, final report to the South Coast Air Quality Management District, 1990.